The Effects of Vegetation Restoration and Season On Soil Enzyme Activity and Microbial Communities in Karst Rocky Desertification Area

Zhang Guo (zhangguo2017@gznu.edu.cn)
Guizhou Normal University https://orcid.org/0000-0001-8098-4879
Chunyan Zheng
Institute of Genetics and Developmental Biology
Zhu Chen
Guizhou University
Jin Wang
Guizhou Normal University
Yanghua Yu
Guizhou Normal University
Ziqi Liu
Guizhou Normal University
Guangbin Yang
Guizhou Normal University
Kangning Xiong
Guizhou Normal University

Research Article

Keywords: community composition, enzyme activity, microbial biomass, soil organic carbon, structural equation model

Posted Date: November 15th, 2021

DOI: https://doi.org/10.21203/rs.3.rs-1034939/v1

Abstract

Aims The process of karst rocky desertification has been closely related to improper land use in southwest China. Now this habitat is the subject of an important ecological restoration project. However, the changes in soil properties and microbial characteristics in response to this vegetation restoration remain poorly understood.

Methods We investigated four vegetation types, including dragon fruit, Chinese pepper, walnut teak, with corn as a control, in southwest China, in 2019. We measured the impacts of these vegetation types on soil properties and microbial biomass, enzyme activity, and microbial community composition (using high-throughput sequencing technology).

Results The different vegetation types had significantly different impacts on soil exchangeable Ca^{2+}, soil organic carbon and available nutrients. The vegetation types also significantly affected microbial biomass. Soil enzyme activity, including b-1,4-glucosidase, b-1,4-N-acetylglucosaminidase, alkaline phosphatase, and catalase, were significantly different among vegetation types. All vegetation types were dominated by the bacterial phyla Acidobacteria, Proteobacteria, and Actinobacteria and the fungal phylum Ascomycota, except for corn which was dominated by the fungal phylum Mucoromycota. Non-metric multidimensional scaling (NMDS) showed that the vegetation type exhibited different microbial b-diversity, especially in winter. The vegetation type, season, and soil properties collectively explained 46% and 59% of soil bacterial and fungal community composition, respectively. The bacterial-fungal interactions under the six vegetation types were distinctly different between summer and winter.

Conclusions Compared with traditional corn, the restoration of natural vegetation partially reversed KRD by improving soil properties, increasing microbial biomass, and differentiating the microbial community structures in the different vegetation types.

1. Introduction

Surface and near-surface karst outcrops occupy 20% of the world's ice-free dry land (Ford and Williams 2013). Karst areas are extremely valuable resources and host a rich variety of plants and animals (Gutiérrez et al. 2014), supply water to 25% of the planet's population (Ford and Williams 2013) and are closely associated with rural poverty (Wang et al. 2019). However, karst rocky desertification (KRD) with degradation of soil ecosystems and plant communities has occurred in many countries and regions (Jiang et al. 2014). The exposed karst area in southwest China is one of the world's three largest continuous areas of carbonate rocks (Yuan 2008). It provides a variety of unique ecological niche and is one of the world's 34 biodiversity hotspots (Myers et al. 2000). However, it possesses 10 million ha of KRD due to improper land use (National Forestry and Grassland Administration of China 2018; Jiang et al. 2014). The process of KRD is positively related to vegetation degradation from secondary forest to sparse shrub and grassland, but this degradation could be partly reversed by ecological restoration (Liu et al. 2009). The Chinese "14th Five-Year Plan" (2021–2025) proposes promotion of a comprehensive and scientific management plan to tackle KRD. The process of halting KRD had previously involved ecological restoration techniques to restore degraded ecosystems (Yuan 2008).

Soil microorganisms are the key drivers of biogeochemical processes in the atmosphere, hydrosphere, lithosphere, and biosphere (Bardgett et al. 2008; Chen et al. 2018; Eugene 2011). Using 16S rRNA amplicon metagenomics, Avitia et al. (2021) showed that the composition of the soil microbial community changed when grasslands transitioned to woody plant cover. Zhao et al. (2018) found that areas afforested with *Robinia pseudoacacia* over a 42, 27 and 17 year chronosequence increased their microbial diversity and altered community structure compared to farmland. In non-karst ecosystems, microbial community structures and activities are also affected by climate (temperature and precipitation) (Shi et al. 2020; Zhou et al. 2016), land use (Tian et al. 2017), fertilization (Zhao et al. 2020), gradient (Shen et al. 2020), elevated atmospheric CO_2 (Fang et al. 2015), organic input (Sun et al. 2020; Zhou et al. 2016), and invasive plant species (Wang et al. 2017). Alterations in microbial community structures corresponded with changes in the microbial substrate due to numerous environmental factors, especially to the fraction of soil organic carbon (SOC) (Zhao et al. 2018).

The microbial communities and activity in karst ecosystems are also sensitive to changes in environmental factors (Chen et al. 2019; Tang et al. 2019). Using ecoenzymatic stoichiometry methodology, Chen et al. (2019) showed that the soil microbes in karst ecosystems are more limited by carbon (C) and phosphorus (P), than by nitrogen (N) levels, compared with non-karst ecosystems. Furthermore, Tang et al. (2019) found that six bacterial groups were significantly correlated with soil Ca^{2+} and available P, suggesting a Ca^{2+}-driven bacterial response mechanism as KRD progressed. Karst rocky desertification reduces the amount of SOC, resulting in a decrease in soil microbial biomass (Li et al. 2013). Zhu et al. (2012) showed that bacterial diversity, fungal diversity, and metabolic diversity were significantly higher in shrublands, secondary forests, and primary forests than in farmlands and grasslands, while the fungal diversity of primary forests was significantly lower than in shrublands and secondary forests. Restoration measures using the tree species *Toona sinensis*, hybrid elephant grass *Pennisetum* spp., and a mixture of *Zenia insignis* and hybrid elephant grass, effectively improved vegetation structure and coverage, and partially restored microbial abundance (Li et al. 2018a). Li et al. (2018b) investigated N functional genes in soil profiles as vegetation recovery progressed and found that active N-acquisition increased as the vegetation recovered. Vegetation restoration increased soil enzyme activity and microbial biomass, before fungi gradually took over as the major decomposers (Hu et al. 2016). Therefore, both KRD and vegetation restoration directly and indirectly affect soil enzyme activity and microbial communities through changes in soil properties.

Due to environmental heterogeneity and discontinuous soil distribution, more articles on the soil microorganisms of non-karst habitats have been published than on the karst ecosystem in China. However, recently more attention has been paid to the eco-environmental issues in the karst ecosystem, especially habitat fragility, the process of KRD, ecological restoration, and ecosystem services. In this study, we investigated the impacts of vegetation restoration using four economically important plants on soil properties, enzyme activity, and microbial biomass and community structure. We aimed to: (1) estimate the effect of vegetation type and season on soil physico-chemical properties; (2) investigate the responses of microbial biomass and enzyme activity to vegetation type and season; and (3) clarify how the vegetation type and season affect soil enzymes, microbial biomass, diversity, and community structure.

2. Materials And Methods

2.1 Study site

The study site is located within the Guanling-Zhenfeng demonstration area for the reduction and control of karst rocky desertification, Guizhou Province, China (25°39'13" ~ 25°41'00" N, 105°36'30" ~ 105°46'30" E). The site is characterized by a humid subtropical monsoon climate with a mean annual temperature of 18.4°C and a mean annual precipitation of 1100 mm, 83% of which falls from May to October. The lithology is dolomitic limestone of the Middle Triassic system, and the soil type is calcareous. This site suffers from serious soil erosion due to anthropogenic disturbance, especially related to cultivation, which has led to KRD, with a rock exposure rate of 70% per year (Li et al. 2020) and a thin, discontinuous soil layer. The native forest cover has diminished (Cheng et al. 2020) and some economically important revegetation has now been carried out to reverse the effects of KRD, including the planting of dragon fruit (*Hylocereus undatus*), Chinese pepper (*Zanthoxylum bungeanum*), walnut (*Carya cathayensis*), teak (*Tectona grandis*), honeysuckle (*Lonicera japonica*), and paper mulberry (*Broussonetia papyrifera*).

2.2 Study design and field sampling

This study sampled soils underneath dragon fruit (DF), walnut (WN), teak (TW), and Chinese pepper growing in depressions (CPD) and on sloping sites (CPS) (Fig. 1). Traditionally farmed corn (*Zea mays*) (CN) growing on a nearby terraced slope served as a comparison. Detailed information on the six sample sites is shown in Table 1. Within each site, six plots were selected with two plots each on the upper, middle, and lower slopes. The upper, middle, and lower slope plots were 10 m apart within a site for the DF, TW and CN, and 5 m apart for the WN, and CPD and CPS. Five soil samples were collected per plot at a depth of 20 cm, along an S-shaped transect, in June and November 2019, and mixed to form one composite sample.

Table 1
Description of six vegetation types in the karst ecosystems.

Vegetation type	Location	Elevation (m)	Slope angle (°)	Management practice
Dragon fruit	25°40'26" N 105°39'51" E	606~630	14 (terraced slope)	For each dragon fruit, fertilization with 2.5 kg cow dung compost in January and 0.5 kg compound fertilizer in July in each year, biomass harvest.
Chinese pepper in depression	25°39'40" N 105°39'4"E	704	0 (depression)	Fertilization with compound fertilizer (N:P:K= 15:8:12) in February, May and July in each year, no cultivation and biomass harvest.
Corn	25°40'26" N 105°39'57" E	620~638	15 (terraced slope)	Cultivation and fertilization with urea in April and June in each year, biomass harvest.
Walnut	25°39'30" N 105°38'33" E	820~826	13 (terraced slope)	No human disturbance of cultivation, fertilization, biomass discard.
Teakwood	25°40'24" N 105°39'56" E	599~615	12 (terraced slope)	No human disturbance of cultivation and fertilization, biomass discard.
Chinese pepper on slope	25°39'27" N 105°38'35" E	828~840	30 (terraced slope)	Sloping land, fertilization with compound fertilizer (N:P:K= 15:8:12) in February, May and July in each year, no cultivation and biomass discard.

2.3 Analysis of soil physico-chemical properties

The following soil physico-chemical properties were determined using the methods of Bao (2000): soil moisture was measured using an oven-drying method; soil pH was measured in a 1:2.5 (soil:water) mixture using the potentiometric method; exchangeable Ca^{2+} (Ca^{2+}) was measured using the ammonium acetate extraction-atomic absorption spectrophotometer method; SOC was measured using the vitriol acid-potassium dichromate oxidation method; total nitrogen (TN) was measured using the Kjeldahl method; soil NH_4^+-N and NO_3^--N were measured using a continuous flow autoanalyzer following extraction with 2 M KCl with a 1:5 ratio; available phosphorus (AP) was measured using the $NaHCO_3$ method; and available potassium (AK) was analyzed using the flame photometer method (Cui et al. 2018).

2.4 Microbial biomass measurement and enzyme activity assay

Microbial biomass carbon (MBC) and nitrogen (MBN) levels were determined using the chloroform fumigation-extraction method (Joergensen and Brookes 2005). Fresh soil from each composite was sieved (2 mm sieve) and six 25 g subsamples were incubated in the dark at 25 °C for 7 d. Three of these subsamples were fumigating with ethanol-free chloroform and incubated in the dark at 25 °C for 24 h. The remaining three subsamples were mixed with 100

ml 0.5 M K_2SO_4 in a rotatory shaker (200 rpm). The fumigated subsamples were extracted using a similar method to the unfumigated subsamples. All extracts were filtered and analyzed using the potassium dichromate-dilution heat colorimetric method. Extracellular enzyme activity, including C-acquiring β-1,4-glucosidase (BG), N-acquiring β-1,4-N-acetylglucosaminidase (NAG), and organic P-acquiring alkaline phosphatase (AKP), were determined by micro-plate enzyme assay (Cui et al. 2018). Enzyme activity was expressed as nanomoles of substrate released per hour per gram of soil organic matter (nmol g SOM^{-1} h^{-1}). Catalase (CAT) activity was determined using the $KMnO_4$ titration method (Guan 1986).

2.5 Determination of microbial community composition

DNA extraction: all soil samples collected were processed individually. The total DNA was extracted using a MoBioPowerSoil™ DNA Isolation Kit (MO BIO Laboratories Inc., Carlsbad, CA, USA), according to the manufacturer's instructions, and DNA integrity was determined by electrophoresis on a 1% agarose gel. The DNA was quantified using a Qubit2.0 DNA Kit (ThermoFisher Scientific, Waltham, MA USA), according to the manufacturer's instructions.

PCR amplification and Illumina MiSeq sequencing: microbial structure and diversity were analyzed using high-throughput sequencing (Illumina HiSeq 2500, BioMarkerTechnologies Co., Ltd., Beijing, China). DNA quality and quantity were assessed in the ranges 260 nm/280 nm and 260 nm/230 nm. Then, DNA was stored at -80°C until further processing. The bacterial community composition was assessed by sequencing the V3-V4 region of the 16S rRNA gene using the PCR primers 5'-ACTCCTACGGGAGGCAGCA-3' and 5'-GGACTACHVGGGTWTCTAAT-3' (Walters et al., 2016). The fungal internal transcribed spacers (ITS) of the 18S rRNA gene were amplified using the primer sets ITS1 5'-CTTGGTCATTTAGAGGAAGTAA-3' and ITS2 5'- GCTGCGTTCTTCATCGATGC-3' (Mueller et al., 2014). The amplification products from the first PCR step were purified through VAHTSTM DNA Clean Beads for the second round of PCR. Finally, all PCR products were quantified using a Qubit2.0 DNA Kit. The amplicons were sequenced using an Illumina Hiseq 2500. The sequences were initially processed using Prinseq (PRINSEQlite 0.19.5 – http://prinseq.sourceforge.net/) to remove low-quality data and improve the syncretic rates of the subsequent sequence. Split sequences for each sample were merged using FLASH V1.2.7 (Magoc and Salzberg, 2011). UCLUST (version 1.2.22) was used with a cut-off of 97% to cluster the operational taxonomic units (OTUs), and the taxonomic classification was performed using an RDP Classifier (Version 2.2, based on Bergey's taxonomy), with the classification threshold set at 0.8. The sequences were taxonomically identified using a BLASTn search of a curated NCBI database.

2.6 Statistical analyses

All statistical analyses of soil properties and Pearson's correlations were analyzed using the SPSS 20.0 program (SPSS Inc., USA). The significance between vegetation types and seasons was assigned at $P < 0.05$ using two-way analyses of variance (ANOVA) with Tukey's test. The bacterial and fungal community compositions (β-diversity) were assessed using non-metric multidimensional scaling (NMDS) based on Bray-Curtis distances. Permutational multivariate analysis of variance (PERMANOVA) was performed to investigate the effects of vegetation type on the compositions of the bacterial and fungal communities. NMDS and PERMANOVA were performed using the vegan package in R software (Team 2021). Microbial network analysis at the bacterial and fungal OUT level was performed using the MENA platform (http://ieg4.rccc.ou.edu/mena) based on Spearman correlation scores (Spearman's $r > 0.7$ or $r < -0.7$; $P < 0.01$) (Deng et al. 2012). The networks were visualized using the Gephi program, version 0.9.2 (Bastian et al. 2009). We used a structural equation model (SEM) to investigate the direct and indirect influences of vegetation type, season, and soil properties on soil enzyme activity, microbial biomass, Shannon diversity index, and community composition. We constructed a priori SEM based on current knowledge, model modification indices, and stepwise removal of non-significant relationships (de Vries and Bardgett 2016). We used a minimum set of parameters to assess model fit using the multigroup modeling approach with the R package lavaan (Rosseel 2012), including soil properties, enzyme activity, and microbial biomass. We used the first two NMDS axes as proxies for bacterial and fungal community composition. Pearson's correlation heatmaps were constructed using BMKCloud (www.biocloud.net).

3. Results

3.1 Soil physico-chemical properties

The results of the two-way ANOVA showed that the soil properties were significantly different between all vegetation types (Table 2). In both summer and winter, the soil moisture content was between 21.14% – 31.84% under all vegetation types. According to the average pH in the two seasons, the vegetation types were ranked: WN (7.92) > CPD (7.85) > CPS (7.66) > DF (7.64) > CN (7.53) > TW (7.35). In summer, the soil exchangeable Ca^{2+} content was highest under CPD and lowest under CN, while in winter it was highest under DF and lowest under CPS. With respect to SOC and TN contents, the vegetation types followed the order: CPS > WN > CPD > TW > DF > CN. In summer and winter, according to the soil NO_3^-N content, the vegetation types ranked in the order: CN > DF > CPD > CPS > WN > TW. However, regarding the soil NH_4^+-N content, the order was WN or CPS > CN, DF > TW or CPD. In summer and winter, the AP content under CPD was 1.4–8.6 times greater than under the other vegetation types. For all vegetation types, the range of soil AK content was lower than that for AP content. Taking the average value, the soil AK content was the highest at 139 mg/kg under DF and lowest at 74 mg/kg under CPS.

Table 2
Soil physico-chemical properties of six vegetation types in 2019

Vegetation type	Soil moisture (%)	pH	Ca^{2+} (g/kg)	SOC (g/kg)	TN (g/kg)	NH_4^+-N (mg/kg)	NO_3^--N (mg/kg)	AP (mg/kg)	AK (mg/kg)
Summer									
DF	25.27±0.68b	7.68±0.03bc	2.30±0.11ab	11.11±0.82d	1.06±0.10d	0.22±0.03a	4.76±0.98ab	2.12±0.32b	112.32±3.74a
CPD	27.77±0.84ab	7.86±0.05ab	2.62±0.08a	24.33±0.34c	2.20±0.03c	0.19±0.02a	3.48±1.00abc	11.12±1.17a	109.15±6.86a
CN	23.60±1.68b	7.59±0.08c	2.11±0.09b	8.85±0.30d	0.80±0.03d	0.28±0.09a	7.28±1.40a	2.25±0.75b	108.74±4.19a
WN	27.41±0.77ab	7.95±0.02a	2.32±0.09ab	29.02±0.94b	2.65±0.07b	0.41±0.07a	2.12±0.70bc	2.52±0.62b	105.07±11.65
TW	24.35±2.37b	7.48±0.07c	2.38±0.20ab	11.66±0.16d	1.05±0.02d	0.20±0.08a	0.62±0.07c	1.20±0.23b	88.03±6.46ab
CPS	31.84±1.48a	7.67±0.06bc	2.12±0.04ab	37.49±2.14a	3.36±0.21a	0.29±0.09a	2.19±0.79bc	2.62±0.89b	73.09±9.81b
Winter									
DF	25.5±0.96ab	7.60±0.05ab	2.80±0.10a	11.41±0.55c	1.41±0.15b	2.56±0.07a	5.83±0.77b	3.02±0.35b	166.35±7.79a
CPD	29.68±1.26a	7.85±0.03a	2.32±0.12ab	25.57±0.86b	2.97±0.16a	2.55±0.07a	4.59±0.41bc	7.25±0.96a	146.85±9.6ab
CN	27.83±1.65a	7.47±0.27ab	2.48±0.16a	10.60±0.50c	1.30±0.03b	2.67±0.15a	8.14±0.28a	2.43±0.37b	143.22±5.76a
WN	29.95±1.09a	7.9±0.00a	1.62±0.14cd	30.22±1.53b	3.39±0.08a	2.70±0.10a	2.75±0.10d	2.48±0.26b	96.97±9.13cd
TW	21.14±2.10b	7.23±0.13b	1.88±0.10bc	16.33±2.25c	1.54±0.20b	2.40±0.05a	2.44±0.01d	1.70±0.06b	122.99±13.89
CPS	29.62±1.12a	7.66±0.08ab	1.30±0.10d	39.28±1.64a	3.96±0.61a	2.79±0.15a	3.42±0.30cd	3.03±0.50b	75.60±5.86d
Two-way ANOVA									
Vegetation type	*ns*	***	***	***	***	*	***	***	***
Season	***	*ns*	***	*	***	***	**	*ns*	***
Vegetation type × Season	*ns*	*ns*	***	*ns*	*ns*	*ns*	*ns*	**	**

DF dragon fruit, *CPD* Chinese pepper in depression, *CN* corn, *WN* walnut, *TW* teakwood, *CPS* Chinese pepper on slope, *Ca^{2+}* exchangeable Ca^{2+}, *SOC* soil orgar carbon, *TN* total nitrogen, *AP* available phosphorus, *AK* available potassium. Values (Means ± standard error) followed by the different letter are significantly different within columns in the same season (*$P < 0.05$*). *, **, and *** indicate significant differences at *$P < 0.05$*, *$P < 0.01$*, and *$P < 0.001$*, respectively. *ns* mear no significance.

Except for soil pH and AP content, soil properties changed significantly with the seasons (Table 2). Under all vegetation types, the soil pH declined by 0.02–3.37% from summer to winter. Soil Ca^{2+} content increased by 22% and 17% under DF and CN, respectively, but decreased by 11% – 39% under the other vegetation types. The contents of soil SOC and TN both increased under all vegetation types, notably by 20% for SOC and 63% for TN under CN. Similarly, under TW the soil NO_3-N and NH_4^+-N contents increased by 12% – 296% and 559% – 1217%, respectively. From summer to winter, the soil AP content increased by 43%, 42%, and 16% under DF, TW, and CPS, respectively, and decreased by 35% under CPS. Meanwhile, the soil AK content increased by 32–48% under CN, CPD and CPS, TW, and DF, and decreased by 8% under WN. The interactions between vegetation type and season were significant for soil Ca^{2+}, AP, and AK contents, but were not significant for the other soil properties.

3.2 Soil microbial biomass and enzyme activity

Vegetation type had a very significant impact on soil MBC and MBN (Table 3). The soil MBC and MBN contents under CPD and CPS, and WN were higher than those under TW, DF, and CN. In summer, the soil MBC under CPS was the highest, and 2.77 times the lowest value under DF. Meanwhile, soil MBN under WN was the highest and 1.3 times greater than under TW. Compared to summer, the soil MBC in winter was significantly lower by 23–26% under all vegetation types except for TW, which increased by 0.72%. Meanwhile, soil MBN decreased significantly by 62% – 83% under all vegetation types. The ratios of MBC/SOC, MBN/TN, and MBC/MBN showed significant differences among the six vegetation types and the two seasons ($P < 0.01$, Table S1). The MBN/TN ratio was also significantly affected by the interaction of vegetation type and season ($P < 0.001$, Table S1).

Table 3
Soil microbial biomass and enzyme activities of six vegetation types in 2019

Vegetation type	MBC (mg/kg)	MBN (mg/kg)	BG (nmol/g/h)	NAG (nmol/g/h)	AKP (nmol/g/h)	CAT (ml/g/30min)
Summer						
DF	130.69±6.01c	50.7±7.98b	309.76±6.27b	266.36±11.61b	346.38±9.19ab	11.34±0.01a
CPD	266.7±17.66b	89.16±3.05a	98.90±12.48d	53.72±7.46c	123.73±9.23c	11.27±0.01a
CN	132.12±8.92c	55.14±2.27b	413.38±11.99a	344.04±36.10ab	521.41±76.02a	11.35±0.01a
WN	356.7±21.15a	93.33±6.15a	102.93±4.14cd	25.69±3.96c	278.28±21.00bc	11.21±0.02a
TW	162.83±12.36c	40.61±1.28b	355.40±24.6ab	406.38±40.33a	523.55±68.15a	11.38±0.01a
CPS	361.68±39.77a	79.29±6.2a	187.22±39.57c	122.70±36.95c	213.43±53.77bc	10.97±0.10b
Winter						
DF	99.75±15.47b	11.42±2.33bc	414.84±30.42a	1204.40±87.49a	1058.3±136.69ab	11.31±0.01a
CPD	203.99±4.41ab	29.92±2.65a	106.21±3.60c	463.37±47.29b	338.65±17.47c	11.28±0.01ab
CN	97.48±7.27b	9.27±0.4c	406.40±70.24a	1246.01±122.96a	1435.61±185.45a	11.30±0.00a
WN	275.05±15.75a	35.19±4.28a	81.39±10.75c	337.92±14.22b	300.49±15.21c	11.25±0.01c
TW	164±42.33ab	13.06±3.14bc	275.18±20.19ab	1286.76±99.89a	1418.18±147.96a	11.29±0.02ab
CPS	261.73±42.89a	23.04±3.75ab	173.79±23.03bc	495.47±174.82b	775.04±121.44bc	11.25±0.00c
Two-way ANOVA						
Vegetation type	***	***	***	***	***	***
Season	***	***	*ns*	***	***	*ns*
Vegetation type × Season	*ns*	**	*ns*	***	***	***

DF dragon fruit, *CPD* Chinese pepper in depression, *CN* corn, *WN* walnut, *TW* teakwood, *CPS* Chinese pepper on slope, *MBC* microbial biomass carbon, *MBN* microbial biomass nitrogen, *BG* β-1,4-glucosidase, *NAG* β-1,4-N-acetylglucosaminidase, *AKP* alkaline phosphatase, *CAT* catalase. Values (Means ± standard error) followed by the different letter are significantly different within columns in the same season ($P < 0.05$). ** and *** indicate significant differences at $P < 0.01$ and $P < 0.001$. *ns* means no significance.

Vegetation type also significantly influenced enzyme activity, including BG, NAG, AKP, and CAT (Table 3). All of the enzyme activities under TW, CN, and DF were generally higher than those under WN, and CPS and CPD. Regarding BG, the enzyme activity ranged from 80–415 nmol g^{-1} h^{-1} in both summer and winter. Compared with summer, enzyme activity was significantly elevated in winter by 34% under DF, but declined by 21% and 23% under WN and TW, respectively. NAG activity was elevated 2.2-, 2.6-, 3-, 3.5-, 7.6-, and 12-fold under TW, CN, CPS, DF, CPD, and WN, respectively. Under all vegetation types, AKP activity was also significantly elevated by 8–263%. In both summer and winter, CAT activity under CPS was significantly lower than under all other vegetation types.

3.3 Microbial community composition and network analysis

In summer, the microbial diversity indexes of bacteria and fungi, including ACE, Chao, and Shannon, showed no significant difference among all vegetation types (Table 4). From summer to winter, the bacterial ACE index declined by 0.56% – 3.98% under all vegetation types except under DF, which increased by 0.65%. The bacterial Chao index increased under DF and CPS, but decreased under the other vegetation types. Under CPD, the bacterial Shannon index significantly increased by 2.6%. For fungi, the Chao index increased by 14% and 12% under CPD and CPS, respectively, but decreased by 11% under CN. The Shannon indexes increased significantly by 46% and 17% under WN and CPS, respectively, but decreased by 28%, 22%, and 17% under DF, CN, and CPD, respectively.

Table 4
The α-diversity index of microbial community of six vegetation types in 2019

Vegetation type	Bacteria			Fungi		
	Ace	Chao	Shannon	Ace	Chao	Shannon
Summer						
DF	1114.32±14.86a	1125.5±12.35a	8.56±0.12a	489.02±37.71a	483.09±38.22a	4.76±0.40a
CPD	1110.54±8.98a	1133.42±12.62a	8.47±0.07a	501.01±47.95a	492.42±44.68a	5.16±0.77a
CN	1118.12±8.59a	1137.36±9.8a	8.45±0.08a	572.46±26.55a	542.96±29.65a	4.53±0.73a
WN	1124.32±14.97a	1137.6±15.38a	8.65±0.05a	461.52±24.54a	454.8±15.84a	3.08±0.49a
TW	1128.2±6.66a	1137.88±7.23a	8.43±0.15a	467.92±16.99a	477.19±15.43a	4.57±0.26a
CPS	1104.98±11.12a	1110.77±12.81a	8.25±0.23a	474.04±16.32a	441.45±9.25a	4.56±0.23a
Winter						
DF	1121.58±6.29a	1138.92±7.47a	8.59±0.10a	512.15±30.81a	487.43±16.75ab	3.45±0.52b
CPD	1091.79±12.12a	1108.68±14.56a	8.69±0.04a	594.51±46.16a	551.15±16.45a	4.29±0.41ab
CN	1103.7±15.66a	1115.04±18.61a	8.47±0.22a	564.59±27.12a	483.69±20.31ab	3.54±0.55b
WN	1101.36±10.29a	1115.06±9.95a	8.75±0.04a	500.23±21.11a	481.55±19.92ab	4.50±0.27ab
TW	1083.35±19.64a	1091.69±22.66a	8.33±0.16a	456.86±38.35a	457.24±31.26b	4.52±0.22ab
CPS	1098.78±13.12a	1112.91±13.96a	8.60±0.05a	500.79±21.07a	501.33±22.49ab	5.36±0.12a
Two-way ANOVA						
Vegetation type	*ns*	*ns*	*ns*	**	*ns*	*ns*
Season	*	*	*ns*	*ns*	*ns*	*ns*
Vegetation type × Season	*ns*	*ns*	*ns*	*ns*	*ns*	*

DF dragon fruit, *CPD* Chinese pepper in depression, *CN* corn, *WN* walnut, *TW* teakwood, *CPS* Chinese pepper on slope. Values (Means ± standard error) followed by the different letter are significantly different within columns in the same season ($P < 0.05$). * and ** indicate significant differences at $P < 0.05$ and $P < 0.01$, respectively. *ns* means no significance.

At the bacterial phylum level, all vegetation types were dominated by Acidobacteria (35% relative abundance), Proteobacteria (25%), and Actinobacteria (15%) (Fig. 2a). The relative abundance of Acidobacteria was highest under CPD (40%) and lowest under TW (29%). Under CN, the relative abundance of Proteobacteria decreased from 31% in summer to 22% in winter, while that of Actinobacteria increased from 10–18% over the same period. The relative abundance of Proteobacteria and Actinobacteria under WN showed the same trend as under CN. However, under CPD, the relative abundance of Proteobacteria increased from 19–26%, accompanied by a decrease in Actinobacteria from 35–30%. At the fungal phylum level, the most abundant phylum was Ascomycota under CPD and CPS, WN, and TW (average: 56%), while Mortierellomycota was most abundant under CN (38%) (Fig. 2b). From summer to winter, the relative abundance of Ascomycota decreased from 67–36%, while that of Mortierellomycota increased from 6–53% under DF. The relative abundance of Mortierellomycota was more than 33% under CN and CPD, but lower than 4% under TW and CPS.

For both bacteria and fungi, the vegetation type led to significant differences in community composition (Fig. 3, $P < 0.001$), and there was a little overlap among the six vegetation types in summer (Fig. 3a and c). The bacterial and fungal community structures changed from summer (Fig. 3a and c) to winter (Fig. 3b and d), and the tighter clustering can be seen in the bar plots in Fig. 3. Due to their greater artificial disturbance, the Bray-Curtis distance between DF and CN was closer than among the other vegetation types, especially in winter (Fig. 3b and d). Meanwhile, the distance between CPD and CPS was greater than that between WN and CPS due to locational differences in Chinese pepper planting. Therefore, the effect of vegetation type on the composition of the bacterial and fungal communities was greater in winter than in summer, based on the larger PERMANOVA R2 values (Fig. 3).

We then performed network analyses to assess the impact of vegetation type and season on microbial interactions. The soil microbial network patterns differed among the six vegetation types and showed clear changes from summer to winter (Fig. 4a-l, Table S4). The microbial taxa showed higher network connectivity (i.e. network degree) under CN and CPD (Fig. 4c-f) than in other vegetation types. Bacterial taxa had higher network degrees than fungal taxa, especially under CN and CPD in winter (Fig. 4d, f, Table S4). In summer and winter, the average number of nodes under CN (641) was lower than under the other vegetation types (DF 764, CPD 754, WN 746, CPS 734, TW 660), while the average number of links under CN (2333) was lower than under CPD (2764), but higher than under the other vegetation types (Fig. 4, Table S4). The average path distances under CN (5.917) and CPD (5.809) were lower than under the other vegetation types, with values > 7 (Table S4). Moreover, the proportion of negative network edges (mainly representing bacteria-fungi interkingdom correlations) sharply declined from 39.2–8.6% under CPD (Fig. 4c, d) and from 40.3–8.8% under CN (Fig. 4e, f) from summer to winter, respectively.

3.4 Structural equation model (SEM) and Pearson's correlation heatmap

The SEM model was a reasonable fit to our data (Fig. 5). The model showed that 63% and 84% of the variance in the first and second soil fertility NMDS axes was explained by vegetation type, season, and soil moisture (Fig. 5). Soil moisture had significant and positive correlations with the SOC and TN levels (0.555

and 0.598, P < 0.01) (Table S2). The model explained 83% and 71% of the variance in the first and second soil enzyme activity NMDS axes. Season, soil fertility, soil moisture, soil pH and Ca^{2+}, and microbial biomass directly affected soil enzyme activity. The effects of season and soil Ca^{2+} were positive, whereas those of soil fertility, moisture, and soil pH had a negative effect on enzyme activity, which was also supported by the Pearson's correlation (Table S2). The model explained 56% and 75% of the variance of MBC and MBN, respectively, which were directed influenced by season, soil pH, and fertility. Regarding soil fertility, the SOC and TN showed significant correlations with MBC (0.82 and 0.717, P < 0.01, respectively) (Table S2). Vegetation type exerted only an indirect effect on soil microbial biomass and was mediated by soil fertility (NMDS1 0.511 and NMDS2 0.392, P < 0.001) (Fig. 5).

Thirty-five percent of the variance in the bacterial Shannon diversity index was explained by soil pH alone (Fig. 5a, path coefficient = 0.661***). The SEM explained 46% and 58% of the variance in the first and second bacterial community NMDS axes. Soil pH and fertility showed direct positive effects, whereas vegetation type and soil Ca^{2+} showed direct negative effects on bacterial community NMDS1. Vegetation type directly and positively influenced bacterial community NMDS2. Due to direct and indirect effects mediated by soil fertility, vegetation type showed a stronger effect on bacterial community composition than soil pH and Ca^{2+}. The fungal Shannon diversity index was directly and negatively influenced by MBN (-0.659) and soil fertility NMDS2 (0.603) (Fig. 5b). The SEM explained 59% and 42% of the variance of the first and second fungal community NMDS axes. Vegetation type and soil Ca^{2+} showed positive effects while season and soil fertility negatively affected fungal community composition.

For bacterial phyla, the SOC and TN contents showed significant and positive correlations with the abundances of Entotheonellaeota, Armatimonadetes, and Actinobacteria ($P < 0.05$), but were negatively correlated with the abundances of Nitrospirae and Proteobacteria (Fig. 6a, P < 0.05). The soil Ca^{2+}, AP, AK, and NO_3^--N contents were positively correlated with Nitrospirae and Gemmatimonadetes: in particular, the NO_3^--N content was strongly significantly correlated with them (r = 0.69, $P < 0.001$). Meanwhile, the soil Ca^{2+} content was negatively correlated with the abundances of Actinobacteria, Entotheonellaeota, and Firmicutes (r < -0.4, $P < 0.001$). The soil NH_4^+-N content, and the AKP and NAG enzyme activities, were positively correlated with the abundance of Actinobacteria and Chloroflexi, but negatively correlated with the abundance of Proteobacteria. CAT enzyme activity was negatively correlated with the abundance of Rokubacteria and Verrucomicrobia, while the activity of glucosidase was negatively correlated with the abundance of Entotheonellaeota. For the fungal phyla, the soil Ca^{2+}, AP, AK, and NO_3^--N contents were positively correlated with the abundance of Mortierellomycota (Fig. 6b, P < 0.001). However, the soil Ca^{2+}, AK, and NO_3^--N contents showed significant and negative correlations with the abundance of Ascomycota ($P < 0.01$). The soil AP content was positively correlated with the abundances of Chytridiomycota and Zoopagomycota. Glycosidase and NAG activities were positively correlated with the abundance of Glomeromycota.

4. Discussion

4.1 Effects of vegetation type and season on soil physico-chemical properties

Our results showed that some vegetation types, including CPS, CPD, and WN, could alter the physico-chemical properties of soils (Table 2). In both summer and winter, the higher water storage capacities under these vegetation types could prevent soil erosion and desertification (Jiang et al. 2014). The SOC is a perfect proxy for judging improvements in soil quality due to vegetation restoration (Lal 2004). In this study, the SOC was higher under CPS, WN, and CPD, unlike the Ca^{2+} content which did not follow this trend; correlation between SOC and Ca^{2+} was negative and not significant. These results do not agree with other studies, which indicate that higher Ca^{2+} is responsible for SOC stability in karst areas (Li et al. 2018a; Li et al. 2018b). This inconsistency might be explained by differences in management practices, for example the removal of litter and biomass from soils under DF and CN. However, while there was no human intervention in the TW areas, severe water loss and soil erosion under TW did lead to lower SOC contents compared with CPS, WN, and CPD. The significant differences in SOC content among the vegetation types was supported by Liu et al. (2015), who reported that SOC accumulation significantly increased with vegetation succession; i.e., from 29.1 g kg^{-1} in grassland to 73.92 g kg^{-1} in primary forest. Furthermore, Xiao et al. (2017) showed that plantations of economic tree species are probably effective in promoting restoration of soil C sequestration. Therefore, improved C sequestration due to reductions in the progress of KRD can turn karst regions into considerable C sinks (Tong et al. 2018). In this study, the Pearson's correlation between the SOC and TN contents was significantly positive (r = 0.904, $P < 0.01$). Insufficient availability of soil N can easily lead to afforestation failures (Li et al. 2018b). Our results showed that the NH_4^+-N content was more affected by seasonal effects than vegetation type, while the higher observed NO_3^--N values under CN and DF were due to the application of organic and mineral fertilizers. In terrestrial ecosystems, the biogeochemical C, N, and P cycles relate to a combination of primary production, respiration, and decomposition (Delgado-Baquerizo et al. 2013). In this study, the higher AP content under CPD was mainly due to compound fertilizer inputs. It is generally believed that karst farmland in southwest China is highly vulnerable to P loss, and Li et al. (2018b) suggested that optimized combinations of applied inorganic/organic fertilizers could promote P availability. In sum, our results indicated that, compared with CN, the soil properties had been improved under CPS, WN, and CPD but deteriorated under TW. Therefore, although a decrease in human disturbance improved soil properties, some management practices (such as fertilization) could increase the soil nutrients available to economically valuable vegetation.

4.2 Effects of vegetation type and season on soil microbial biomass and enzyme activity

In this study, the contents of soil MBC and MBN were significantly impacted by the vegetation type and season (Table 3). The MBC contents showed a similar trend to SOC, and those under WN, CPS, and CPD were higher than the other three vegetation types. The MBC showed a positive and significant correlation with SOC (r = 0.820, $P < 0.01$, Table S2), a feature also observed by Feng et al. (2016). Liu et al. (2015) studied four vegetation types and found that microbial biomass had a predominant effect on SOC. The MBC/SOC ratio (or MBN/TN) is generally used as an index of substrate quality and the proportion of C (or N) immobilized by microbes (Wen et al. 2014). Therefore, the higher ratios of MBC/SOC (or MBN/TN) observed in this study under CN implied higher mineralization rates of organic matter by the microbial community and higher nutrient utilization rates (Table S1). The MBC/MBN ratio represents the structure and state of a soil microbial community (Joergensen and Brookes 2005). It is widely accepted that the C/N ratio in microbial biomass is about 6.5 for bacteria and 5–17 for fungi (Cleveland and Liptzin 2007). Our results showed that the dominant bacterial effect under CN is greater than under the other

vegetation types in summer. This study also indicated that the soil microbial community is dominated by bacteria in summer (MBC/MBN < 6.5) but by fungi in winter (MBC/MBN > 6.5) (Table S1). Our results also showed that organic inputs, especially high quality organic matter, could favor vegetation types which restore soil microbial biomass.

Soil enzyme activity plays a key role in mineralization and transformation of organic matter, involving C, N, and P cycling in soil ecosystems (Chen et al. 2020; Kumar and Maiti 2011; Liu et al. 2021). In this study, the activities of BG, NAG, AKP, and CAT showed significant differences among the vegetation types ($P < 0.001$, Table 3). The NAG and AKP activities also changed significantly from summer to winter and were significantly affected by the interactions between vegetation type and season ($P < 0.001$). Compared with WN, CPD, and CPS, the activities of BG, NAG, and AKP were higher under CN, TW, and DF and had lower SOC contents. This can be explained by the fact that enzyme activity is strongly affected by the root system when vegetation is intensively planted. Cui et al. (2018) showed that inconsistencies between variations in microbial nutrient ratios and ecoenzyme ratios could be explained by the impacts of root systems. Bell et al. (2014) indicated that the roots of gramineous plants produce more extracellular enzymes to meet their nutrient requirements. Moreover, ecoenzymes produced by roots can enter the soil after root death (Rillig et al. 2007). In this study, soil enzyme activity was directly affected by MBN ($P < 0.01$, Fig. 5). However, NAG activity showed a negative correlation with MBN ($P < 0.01$, Table S2), which was attributed to the fact that NAG decomposes microbial residues to provide available N for soil microorganism and plant growth (Liu et al. 2021). We found that the increases in NAG and AKP activity were higher in winter than in summer, perhaps because of the higher SOC content (Kumar and Maiti 2011). Overall, the enzyme activity responses implied that vegetation restoration could result in different soil nutrient cycles among the six vegetation types.

4.3 Effects of vegetation type and season on the microbial community composition and network

The numbers of bacterial and fungal OTUs differed, but not significantly so, among all vegetation types (Table S3). However, the distribution of bacterial and fungal phyla was clearly different between vegetation types (Fig. 2). Our results showed that Acidobacteria, Proteobacteria and Actinobacteria were dominated under all vegetation types in both seasons (Fig. 2a), as reported by Liao et al. (2018). Liao et al. (2018) also found that some members of the Actinobacteria (e.g., Solirubrobacteraceae) significantly increased their relative abundances following land-use conversion in degraded karst ecosystems. The distribution of bacterial phyla was also affected by the karst terrain. For example, the relative abundance of Acidobacteria on ridges and in depressions were higher than on slopes, while the relative abundance of Proteobacteria showed the opposite trend (Wang et al. 2018). Regarding the fungi, the most abundant phylum under corn was Mortierellomycota, while Ascomycota dominated under the other vegetation types (Fig. 2b). Vegetation restoration therefore clearly altered the relative composition of the soil microbiota, compared with traditional CN planting.

Compared with traditional CN planting, other vegetation types, including WN, CPD, and CPS, significantly increased microbial biomass (Table 2) while showing a similar α-diversity (Table 4). The bacterial Shannon diversity index under WN was higher than under the other vegetation types, perhaps due to lower disturbance and no soil erosion. Liao et al. (2018) implied that the soil bacterial diversity remained unchanged after a 20-year conversion of cropland to Chinese prickly ash orchards. Zhao et al. (2014) studied a progressive succession of secondary vegetation and found that microbial biomass and bacterial biomass were higher during the shrubland phase than in the forest phase due to changes in soil conditions (i.e., reduced pH) and resource availability (i.e., reduced SOC). Hu et al. (2016a) showed that planting of Pepino (*Solanum muricatum*) increased the diversity and abundance of bacterial communities in karst areas. In this study, the microbial diversity was not only affected by vegetation type, but also by substrate and environmental factors.

The vegetation type affected the microbial community composition in both summer and winter (Fig. 3). Avitia et al. (2021) also reported that differences in microbial β-diversity were mainly driven by vegetation type in Arizona. Zheng et al. (2021) found that forest type drove latitudinal differences in AM fungal β-diversity. Regardless of vegetation type, we observed greater variation and more overlap of microbial community composition in summer than in winter (Fig. 3). This difference was perhaps due to the higher temperatures in summer (Fig. 3a and c). This result was consistent with the findings of Shen et al. (2021), which indicated that differences in microbial community composition were greater under warm than cool conditions. Similarly, our results implied that higher summer temperatures increase microbial richness and β-diversity (Table 3 and Fig. 5). In spite of the vegetation species being the same, soils under CPS showed greater bacterial and fungal compositional dissimilarities compared with CPD, than did CPS compared with WN (Fig. 3). This difference appears to be due to location: WN and CPS were found on slopes at similar elevation, while CPD growing in depressions occupied lower elevations. Therefore, in this study in karst areas, microbial β-diversity is affected by spatial heterogeneity, including topography and elevation, as well as by vegetation type and season, a finding supported by other studies (Berthrong et al. 2013; Shen et al. 2021) and which requires further research.

Microbial cooperative networks are critical for plant nutrient availability, growth, and colonization (Tang et al. 2019). Tang et al. (2019) inferred that increases in soil Ca^{2+} content perhaps decrease microbial communication and motility, which can impair the microbial networks in karst areas. The present study of karst rocky desertification areas indicated that bacterial-fungal interaction patterns were distinctly different between the six vegetation types in both summer and winter (Fig. 4). The bacterial taxa present showed higher α-diversity (Table 4) and network connectivity (Fig. 4) than the fungal taxa, according to the dominant vegetation type (Xiong et al. 2021). Our results indicated that the proportion of negative network edges decreased from summer to winter under CPD (Fig. 4c, d) and CN (Fig. 4e,f), primarily due to changes in soil fertility (Table 2) and reduced competition between bacteria and fungi (Xiong et al. 2021).

4.5 Structural equation model and Pearson's correlation under six vegetation types

In karst areas, the microbial community composition is affected by changes in soil properties following vegetation restoration (Li et al. 2018b). Our results showed that some soil properties were significantly correlated with microbial community characteristics (Fig. 6). We found that SOC was positively and significantly correlated with TN level (Table S2), and that the higher SOC and TN contents under WN, CPD, and CPS led to increased microbial biomass (Table 2 and 3). This effect was principally attributed to the coupling of the biogeochemical cycles of C, N, and P in terrestrial ecosystems (Delgado-Baquerizo et al. 2013). However, the higher SOC contents did not lead to higher F/B ratio as implied by other factors, such as root system changes, which may affect microbial community structure (Li et al. 2018b). This study showed that the bacterial phyla Nitrospirae and Gemmatimonadetes were significantly correlated with NO_3^--

N, AP, and AK levels. This result was supported by Wang et al. (2018), who found that variation in the abundance of Nitrospirae is affected by the soil N content. Both N and P are limiting elements in karst areas (Zhang et al. 2015) and are the main factors affecting variations in N-cycling microorganisms (Li et al. 2018c). In karst soils, the C and N contents significantly affected the phoD-harboring bacterial community structure under long-term fertilization (Chen et al. 2018). Therefore, vegetation restoration, including vegetation type and management practices, can alter the composition of microbial communities through changes in soil properties.

In this study, our SEM showed that vegetation restoration and season directly and indirectly affect soil microbial biomass, diversity, and composition mainly through alterations of plant type and soil properties (Fig. 5). Microbial characteristics can be directly affected by soil fertility, which was mainly explained by season and by vegetation type and its cultivation and fertilization (Table 2, Fig. 6 and 5). Soil nutrient availability (e.g., AK, AP, and AN) indirectly affects soil microbial growth, leading to temporal variations in microbial diversity and activity (Yang et al. 2017). We found that both vegetation type and season had a negative effect on soil Ca^{2+} content (Table 2 and Fig. 3). Other studies have also indicated that soil Ca^{2+} content differs between different vegetation types in karst ecosystems (Hu et al. 2021; Xue et al. 2017).

Soil properties significantly affect bacterial community composition during karst vegetation degradation and restoration (Tang et al. 2019). In this study, the vegetation type and soil properties (soil fertility, pH, and Ca^{2+}) directly affected bacterial community composition (Fig. 5). The bacterial community was more responsive to soil pH than the fungal community, as also shown by some other studies (Bahram et al. 2018; Tedersoo et al. 2014; Teng et al. 2021). Rousk et al. (2010) showed that the direct effect of soil pH on bacterial communities is probably due to the narrow pH range for optimal growth in bacteria, contrary to the wider pH range for fungi. Delgado-Baquerizo et al. (2017) showed that soil pH mediates the positive effects of certain microbial taxa on multifunctional resistance to global change. The present study showed a significant and negative effect of soil Ca^{2+} content on bacterial community composition (Fig. 5), in agreement with Tang et al. (2019), indicating that increases in soil Ca^{2+} content alter bacterial community abundance and composition in karst areas.

In this study, vegetation type and soil Ca^{2+} had direct positive effects on fungal community composition, while season and soil fertility had negative effects (Fig. 3). The seasonal effects on fungal communities were perhaps directly driven by temperature and precipitation. These climatic factors determine fungal survival and colonization (Teng et al. 2021). The SEM explained 34.7% and 19.6% of the Shannon diversity index found in our study for bacteria and fungi, respectively (Fig. 5). Soil pH was the only contributor to the bacterial Shannon diversity index (0.661***) (Fig. 5). However, bacterial and fungal β-diversity showed significant differences among the six vegetation types, especially in winter (Fig. 3). Our results implied that microbial α-diversity may be improved by increasing aboveground diversity using mixed planting of different vegetation types.

Conclusions

In this study, we investigated the impacts of four restored vegetation types in Guizhou province, southwest China, in 2019. The soils under the vegetation types contained significantly different amounts of SOC, TN, soil exchangeable Ca^{2+}, and available nutrients. The soil properties changed significantly from summer to winter, except for soil pH and AP content. The microbial biomass under WN, CPS, and CPD was greater than under DF, TW, and traditional CN. Soil enzyme activity, including BG, NAG, AKP, and CAT, were significantly different among the vegetation types ($P < 0.001$). The bacterial and fungal diversity indexes, including the ACE, Chao, and Shannon indexes, showed no significant differences among all of the vegetation types. All vegetation types were dominated by the bacterial phyla Acidobacteria, Proteobacteria, and Actinobacteria and the fungal phylum Ascomycota, except for soils under CN, which were dominated by the fungal phylum Mucoromycota. The bacterial-fungal networks were distinctly different among the six vegetation types. Vegetation type, season, and soil properties collectively explained 46% and 59% of the bacterial and fungal community compositions, respectively. Soil pH and fertility exerted the strongest direct effects on bacterial communities. The SOC and TN contents were significantly positively correlated with the abundances of Entotheonellaeota, Armatimonadetes, and Actinobacteria ($P < 0.05$). The soil exchangeable Ca^{2+} content exerted direct effects on both the bacterial and fungal communities. Therefore, vegetation restoration partly reversed the effects of KRD by improving soil properties, increasing microbial biomass, and differentiating the microbial community structures compared with traditional CN vegetation.

Declarations

Acknowledgements

This work was supported by the World First-class Academic Discipline Construction Project of Guizhou Province (Qianjiaoke YF(2019)125), the Joint Fund of the National Natural Science Foundation of China and the Karst Science Research Center of Guizhou province (Grant No. U1812401), the Guizhou Science and Technology Fund Project (Qiankehe LH (2017)7372), and the Science Foundation for Doctor of Guizhou Normal University (110904/0517058). We thank International Science Editing (http://www.internationalscienceediting.com) for editing this manuscript.

Compliance with ethical standards

Conflict of interest The authors declare that they have no conflicts of interest.

References

1. Avitia M, Barrón-Sandoval A, Hernández-Terán A et al (2021) Soil microbial composition and carbon mineralization are associated with vegetation type and temperature regime in mesocosms of a semiarid ecosystem. FEMS Microbiol Lett 368. https://doi.org/10.1093/femsle/fnab012
2. Bahram M, Hildebrand F, Forslund SK et al (2018) Structure and function of the global topsoil microbiome. Nature 560:233–237. https://doi.org/10.1038/s41586-018-0386-6
3. Bao SD (2000) Soil and agricultural chemical analysis, Third edn. China Agriculture Press, Beijing

4. Bardgett RD, Freeman C, Ostle NJ (2008) Microbial contributions to climate change through carbon cycle feedbacks. ISME J 2:805–814
5. Bastian M, Heymann S, Jacomy M (2009) Gephi: an open source software for exploring and manipulating networks. Third international AAAI conference on weblogs and social media
6. Bell CW, Tissue DT, Loik ME, Wallenstein MD, Acosta - Martinez V, Erickson RA, Zak JC (2014) Soil microbial and nutrient responses to 7 years of seasonally altered precipitation in a Chihuahuan Desert grassland. Glob Change Biol 20:1657–1673. https://doi.org/10.1111/gcb.12418
7. Berthrong ST, Buckley DH, Drinkwater LE (2013) Agricultural management and labile carbon additions affect soil microbial community structure and interact with carbon and nitrogen cycling. Microb Ecol 66:158–170. https://doi.org/10.1007/s00248-013-0225-0
8. Burns RG, DeForest JL, Marxsen J, Sinsabaugh RL, Stromberger ME, Wallenstein MD, Weintraub MN, Zoppini A (2013) Soil enzymes in a changing environment: Current knowledge and future directions. Soil Biol Biochem 58:216–234. https://doi.org/10.1016/j.soilbio.2012.11.009
9. Chen H, Li D, Mao Q, Xiao K, Wang K (2019) Resource limitation of soil microbes in karst ecosystems. Sci Total Environ 650:241–248. https://doi.org/10.1016/j.scitotenv.2018.09.036
10. Chen H, Li D, Xiao K, Wang K (2018) Soil microbial processes and resource limitation in karst and non-karst forests. Funct Ecol 32:1400–1409. https://doi.org/10.1111/1365-2435.13069
11. Chen W, Zhou H, Wu Y, Wang J, Zhao Z, Li Y, Qiao L, Chen K, Liu G, Xue S (2020) Direct and indirect influences of long-term fertilization on microbial carbon and nitrogen cycles in an alpine grassland. Soil Biol Biochem 149:107922. https://doi.org/10.1016/j.soilbio.2020.107922
12. Cheng C, Li Y, Long M, Gao M, Zhang Y, Lin J, Li X (2020) Moss biocrusts buffer the negative effects of karst rocky desertification on soil properties and soil microbial richness. Plant Soil https://doi.org 10.1007/s11104-020-04602-4
13. Cleveland CC, Liptzin D (2007) C:N:P stoichiometry in soil: is there a “Redfield ratio” for the microbial biomass? Biogeochemistry 85:235–252. https://doi.org/10.1007/s10533-007-9132-0
14. Cui Y, Fang L, Guo X, Wang X, Zhang Y, Li P, Zhang X (2018) Ecoenzymatic stoichiometry and microbial nutrient limitation in rhizosphere soil in the arid area of the northern Loess Plateau, China. Soil Biol Biochem 116:11–12. https://doi.org/10.1016/j.soilbio.2017.09.025
15. Delgado-Baquerizo M, Maestre FT, Gallardo A et al (2013) Decoupling of soil nutrient cycles as a function of aridity in global drylands. Nature 502:672–676. https://doi.org/10.1038/nature12670
16. Delgado-Baquerizo M, Eldridge DJ, Ochoa V, Gozalo B, Singh BK, Maestre FT (2017) Soil microbial communities drive the resistance of ecosystem multifunctionality to global change in drylands across the globe. Ecol Lett 20:1295–1305. https://doi.org/10.1111/ele.12826
17. Deng Y, Jiang Y-H, Yang Y, He Z, Luo F, Zhou J (2012) Molecular ecological network analyses. BMC Bioinformatics 13:113. https://doi.org/10.1186/1471-2105-13-113
18. de Vries FT, Bardgett RD (2016) Plant community controls on short-term ecosystem nitrogen retention. New Phytol 210:861–874. https://doi.org/10.1111/nph.13832
19. Eugene LM (2011) Microorganisms and their roles in fundamental biogeochemical cycles. Curr Opin Biotechnol 22:456–464. https://doi.org/10.1016/j.copbio.2011.01.008
20. Fang H, Cheng S, Lin E, Yu G, Niu S, Wang Y, Xu M, Dang X, Li L, Wang L (2015) Elevated atmospheric carbon dioxide concentration stimulates soil microbial activity and impacts water-extractable organic carbon in an agricultural soil. Biogeochemistry 122:253–267. https://doi.org/10.1007/s10533-014-0039-2
21. Feng S, Huang Y, Ge Y, Su Y, Xu X, Wang Y, He X (2016) Variations in the patterns of soil organic carbon mineralization and microbial communities in response to exogenous application of rice straw and calcium carbonate. Sci Total Environ 571:615–623. http://dx.doi.org/10.1016/j.scitotenv.2016.07.029
22. Ford D, Williams PD (2013) Karst hydrogeology and geomorphology. John Wiley & Sons
23. Guan S (1986) Soil enzymes and study method. China Agriculture Press, Beijing
24. Gutiérrez F, Parise M, De Waele J, Jourde H (2014) A review on natural and human-induced geohazards and impacts in karst. Earth Sci Rev 138:61–88. https://doi.org/10.1016/j.earscirev.2014.08.002
25. Hu J, Yang H, Long X, Liu Z, Rengel Z (2016a) Pepino (Solanum muricatum) planting increased diversity and abundance of bacterial communities in karst area. Sci Rep 6:21938. https://doi.org/10.1038/srep21938
26. Hu N, Li H, Tang Z, Li Z, Tian J, Lou Y, Li J, Li G, Hu X (2016b) Community diversity, structure and carbon footprint of nematode food web following reforestation on degraded Karst soil. Sci Rep 6:28138. https://doi.org/10.1038/srep28138
27. Hu P, Zhang W, Li D, Zhao Y, Zhao J, Xiao J, Wu F, He X, Luo Y, Wang KL (2021) Soil carbon accumulation with increasing temperature under both managed and natural vegetation restoration in calcareous soils. Sci Total Environ 767:145298. https://doi.org/10.1016/j.scitotenv.2021.145298
28. Jiang Z, Lian Y, Qin X (2014) Rocky desertification in Southwest China: Impacts, causes, and restoration. Earth Sci Rev 132:1–12. https://doi.org/10.1016/j.earscirev.2014.01.005
29. Joergensen RG, Brookes PC (2005) Quantification of soil microbial biomass by fumigation-extraction. Monitoring and Assessing Soil Bioremediation. Springer, pp 281–295
30. Klindworth A, Pruesse E, Schweer T, Peplies J, Quast C, Horn M, Glöckner FO (2013) Evaluation of general 16S ribosomal RNA gene PCR primers for classical and next-generation sequencing-based diversity studies. Nucleic Acids Res 41:e1
31. Kumar S, Maiti S (2011) Soil phosphatase activity in natural and mined soil – A review.Ecology and Environment31

32. Lal R (2004) Soil carbon sequestration impacts on global climate change and food security. Science 304:1623–1627. https://doi.org/10.1126/science.1097396
33. Li C, Xiong K, Wu G (2013) Process of biodiversity research of Karst areas in China. Acta Ecol Sin 33:192–200. http://dx.doi.org/10.1016/j.chnaes.2013.05.005
34. Li D, Liu J, Chen H, Zheng L, Wang K (2018a) Soil microbial community responses to forage grass cultivation in degraded karst soils, southwest China. Land Degradation & Development 29:4262–4270. https://doi.org/10.1002/ldr.3188
35. Li D, Wen L, Jiang S, Song T, Wang K (2018b) Responses of soil nutrients and microbial communities to three restoration strategies in a karst area, southwest China. J Environ Manage 207:456–464. https://doi.org/10.1016/j.jenvman.2017.11.067
36. Li D, Zhang X, Green SM, Dungait JAJ, Wen X, Tang Y, Guo Z, Yang Y, Sun X, Quine TA (2018c) Nitrogen functional gene activity in soil profiles under progressive vegetative recovery after abandonment of agriculture at the Puding Karst Critical Zone Observatory, SW China. Soil Biol Biochem 125:93–102. https://doi.org/10.1016/j.soilbio.2018.07.004
37. Li Y, Liu Z, Liu G, Xiong K, Cai L (2020) Dynamic variations in soil moisture in an epikarst fissure in the karst rocky desertification area. J Hydrol 591:125587. https://doi.org/10.1016/j.jhydrol.2020.125587
38. Liao H, Zheng C, Li J, Long J (2018) Dynamics of soil microbial recovery from cropland to orchard along a 20-year chronosequence in a degraded karst ecosystem. Sci Total Environ 639:1051–1059. https://doi.org/10.1016/j.scitotenv.2018.05.246
39. Liu C, Lang Y, Li S, Piao H, Tu C, Liu T, Zhang W, Zhu S (2009) Researches on biogeochemical processes and nutrient cycling in karstic ecological systems, southwest China: A review. Earth Sci Front 16:1–12. (in China)
40. Liu S, Zhang W, Wang K, Pan F, Yang S, Shu S (2015) Factors controlling accumulation of soil organic carbon along vegetation succession in a typical karst region in Southwest China. Sci Total Environ 521–522:52–58. http://dx.doi.org/10.1016/j.scitotenv.2015.03.074
41. Liu Z, Liu X, Wu X, Bian R, Liu X, Zheng J, Zhang X, Cheng K, Li L, Pan G (2021) Long-term elevated CO2 and warming enhance microbial necromass carbon accumulation in a paddy soil. Biol Fertil Soils. https://doi.org/10.1007/s00374-021-01557-1
42. Magoč T, Salzberg SL (2011) FLASH: fast length adjustment of short reads to improve genome assemblies. Bioinformatics 27:2957–2963
43. Mueller RC, Paula FS, Mirza BS, Rodrigues JLM, Nüsslein K, Bohannan BJM (2014) Links between plant and fungal communities across a deforestation chronosequence in the Amazon rainforest. ISME J 8:1548–1550. https://doi.org/10.1038/ismej.2013.253
44. Myers N, Mittermeier RA, Mittermeier CG, da Fonseca GAB, Kent J (2000) Biodiversity hotspots for conservation priorities. Nature 403:853–858. https://doi.org/10.1038/35002501
45. National Forestry and Grassland Administration of China (2018) 2018 Bulletin on the rocky desertification status of karst areas in China
46. Rosseel Y (2012) Lavaan: An R package for structural equation modeling and more. Version 0.5–12 (BETA). J Stat Softw 48:1–36
47. Rousk J, Baath E, Brookes PC, Lauber CL, Lozupone C, Caporaso JG, Knight R, Fierer N (2010) Soil bacterial and fungal communities across a pH gradient in an arable soil. ISME J 4:1340–1351
48. Shen C, Gunina A, Luo Y, Wang J, He J-Z, Hemp A, Classen A, Ge Y (2020) Contrasting patterns and drivers of soil bacterial and fungal diversity across a mountain gradient. Environ Microbiol 22. https://doi.org/10.1111/1462-2920.15090
49. Shen C, He J, Ge Y (2021) Seasonal dynamics of soil microbial diversity and functions along elevations across the treeline. Sci Total Environ 794:148644. https://doi.org/10.1016/j.scitotenv.2021.148644
50. Shi Y, Zhang K, Li Q, Liu X, He J, Chu H (2020) Interannual climate variability and altered precipitation influence the soil microbial community structure in a Tibetan Plateau grassland. Sci Total Environ 714:136794. https://doi.org/10.1016/j.scitotenv.2020.136794
51. Sun K, Han L, Yang Y, Xia X, Yang Z, Wu F, Li F, Feng Y, Xing B (2020) Application of hydrochar altered soil microbial community composition and the molecular structure of native soil organic carbon in a paddy soil. Environ Sci Technol 54:2715–2725. https://doi.org/10.1021/acs.est.9b05864
52. Tang J, Tang X, Qin Y, He Q, Yi Y, Ji Z (2019) Karst rocky desertification progress: Soil calcium as a possible driving force. Sci Total Environ 649:1250–1259. https://doi.org/10.1016/j.scitotenv.2018.08.242
53. Team RC (2021) R: A language and environment for statistical computing. In: RFfS Computing (ed), Vienna, Austria
54. Tedersoo L, Bahram M, Põlme S et al (2014) Global diversity and geography of soil fungi. Science 346:1256688. https://doi.org/10.1126/science.1256688
55. Teng J, Tian J, Barnard R, Yu G, Kuzyakov Y, Zhou J (2021) Aboveground and belowground plant traits explain latitudinal patterns in topsoil fungal communities from tropical to cold temperate forests. Front Microbiol 12:633751. https://doi.org/10.3389/fmicb.2021.633751
56. Tian Q, Taniguchi T, Shi W-Y, Li G, Yamanaka N, Du S (2017) Land-use types and soil chemical properties influence soil microbial communities in the semiarid Loess Plateau region in China. Sci Rep 7:45289. https://doi.org/10.1038/srep45289
57. Tong X, Brandt M, Yue Y, Horion S, Wang K, Keersmaecker WD, Tian F, Schurgers G, Xiao X, Luo Y, Chen C, Myneni R, Shi Z, Chen H, Fensholt R (2018) Increased vegetation growth and carbon stock in China karst via ecological engineering. Nature Sustainability 1:44–50. https://doi.org/10.1038/s41893-017-0004-x
58. Wang C, Li W, Shen T, Cheng W, Yan Z, Yu L (2018) Influence of soil bacteria and carbonic anhydrase on karstification intensity and regulatory factors in a typical karst area. Geoderma 313:17–24. https://doi.org/10.1016/j.geoderma.2017.10.016
59. Wang C, Zhou J, Liu J, Du D (2017) Responses of soil N-fixing bacteria communities to invasive species over a gradient of simulated nitrogen deposition. Ecol Eng 98:32–39. https://doi.org/10.1016/j.ecoleng.2016.10.073

60. Wang K, Zhang C, Chen H, Yue Y, Zhang W, Zhang M, Qi X, Fu Z (2019) Karst landscapes of China: patterns, ecosystem processes and services. Landscape Ecol 34:2743–2763. https://doi.org/10.1007/s10980-019-00912-w
61. Wen L, Lei P, Xiang W, Yan W, Liu S (2014) Soil microbial biomass carbon and nitrogen in pure and mixed stands of Pinus massoniana and Cinnamomum camphora differing in stand age. For Ecol Manag 328:150–158. https://doi.org/10.1016/j.foreco.2014.05.037
62. Xiao K, He T, Chen H, Peng W, Song T, Wang K, Li D (2017) Impacts of vegetation restoration strategies on soil organic carbon and nitrogen dynamics in a karst area, southwest China. Ecol Eng 101:247–254. http://dx.doi.org/10.1016/j.ecoleng.2017.01.037
63. Xiong C, Singh B, He J, Han Y, Li P, Wan L, Meng G, Liu S, Wang J, Wu C, Ge A, Zhang L (2021) Plant developmental stage drives the differentiation in ecological role of the maize microbiome. Microbiome 9. https://doi.org/10.1186/s40168-021-01118-6
64. Xue L, Ren H, Li S, Leng X, Yao X (2017) Soil bacterial community structure and co-occurrence pattern during vegetation restoration in karst rocky desertification area. Front Microbiol 8:2377
65. Yang W, Guo Y, Wang X, Chen C, Hu Y, Cheng L, Gu S, Xu X (2017) Temporal variations of soil microbial community under compost addition in black soil of Northeast China. Appl Soil Ecol 121:214–222
66. Yuan D (2008) Global view on karst rock desertification and integrating control measures and experiences of China. Pratacul Tural Science 25:19–25. (in China)
67. Zhang W, Zhao J, Pan F, Li D, Chen H, Wang K (2015) Changes in nitrogen and phosphorus limitation during secondary succession in a karst region in southwest China. Plant Soil 391:77–91. https://doi.org/10.1007/s11104-015-2406-8
68. Zhao FZ, Ren CJ, Zhang L, Han XH, Yang GH, Wang J (2018) Changes in soil microbial community are linked to soil carbon fractions after afforestation. Eur J Soil Sci 69:370–379. https://doi.org/10.1111/ejss.12525
69. Zhao J, Li S, He X, Liu L, Wang K (2014) The soil biota composition along a progressive succession of secondary vegetation in a karst area. PLoS ONE 9:e112436. https://doi.org/10.1371/journal.pone.0112436
70. Zhao Z, He J, Quan Z, Wu C, Sheng R, Zhang L, Geisen S (2020) Fertilization changes soil microbiome functioning, especially phagotrophic protists. Soil Biol Biochem 148:107863. https://doi.org/10.1016/j.soilbio.2020.107863
71. Zheng Y, Chen L, Ji N, Wang YL, Gao C, Jin SS, Hu H, Huang Z, He JZ, Guo L, Powell J (2021) Assembly processes lead to divergent soil fungal communities within and among twelve forest ecosystems along a latitudinal gradient. New Phytol 231. https://doi.org/10.1111/nph.17457
72. Zhou G, Zhang J, Chen L, Zhang C, Yu Z (2016) Temperature and straw quality regulate the microbial phospholipid fatty acid composition associated with straw decomposition. Pedosphere 26:386–398. http://dx.doi.org/10.1016/S1002-0160(15)60051-0
73. Zhu H, He X, Wang K, Su Y, Wu J (2012) Interactions of vegetation succession, soil bio-chemical properties and microbial communities in a Karst ecosystem. Eur J Soil Biol 51:1–7. http://dx.doi.org/10.1016/j.ejsobi.2012.03.003

Figures

Figure 1

The study sampled soils underneath dragon fruit (DF), walnut (WN), teak (TW), and Chinese pepper growing in depressions (CPD) and on sloping sites (CPS)

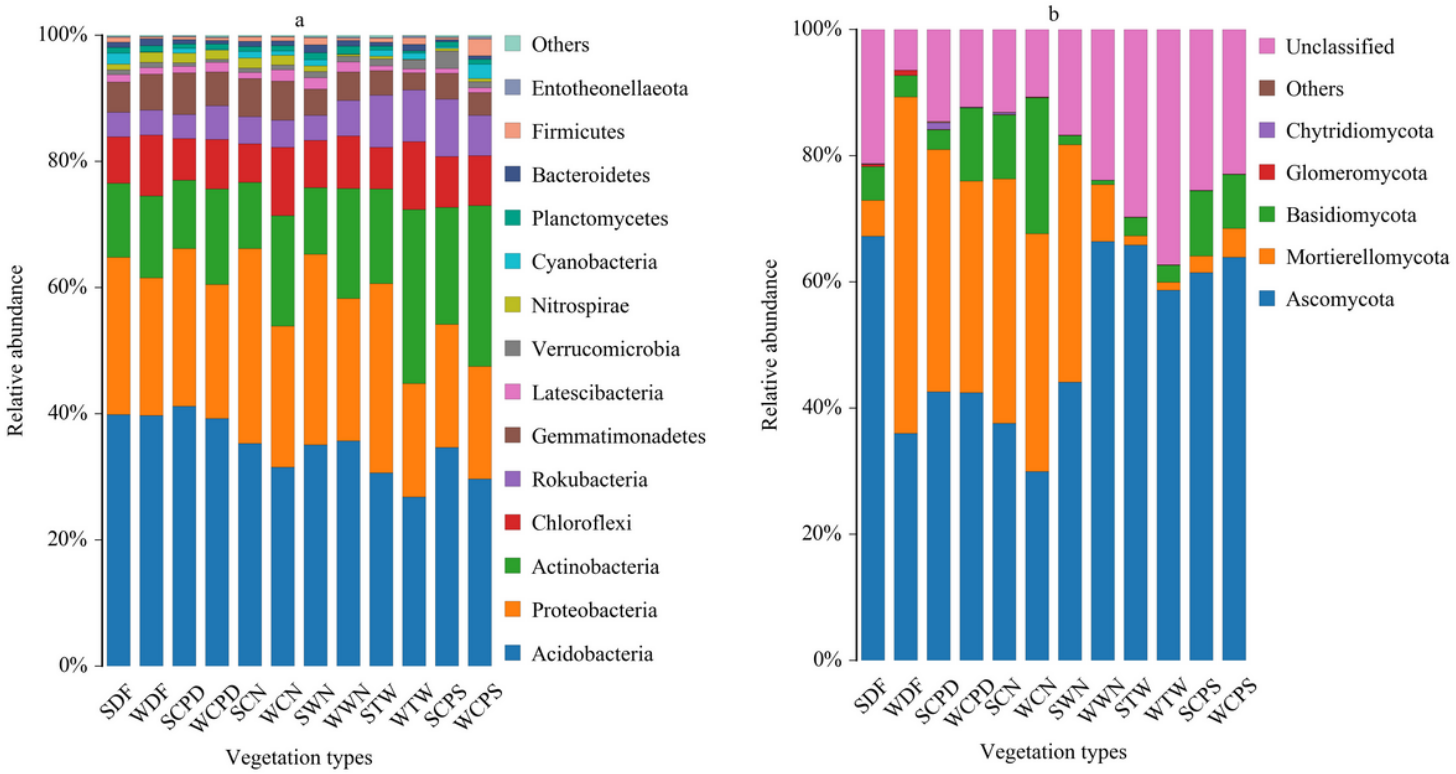

Figure 2

At the bacterial phylum level, all vegetation types were dominated by Acidobacteria (35% relative abundance), Proteobacteria (25%), and Actinobacteria (15%) (Fig. 2a). At the fungal phylum level, the most abundant phylum was Ascomycota under CPD and CPS, WN, and TW (average: 56%), while Mortierellomycota was most abundant under CN (38%) (Fig. 2b).

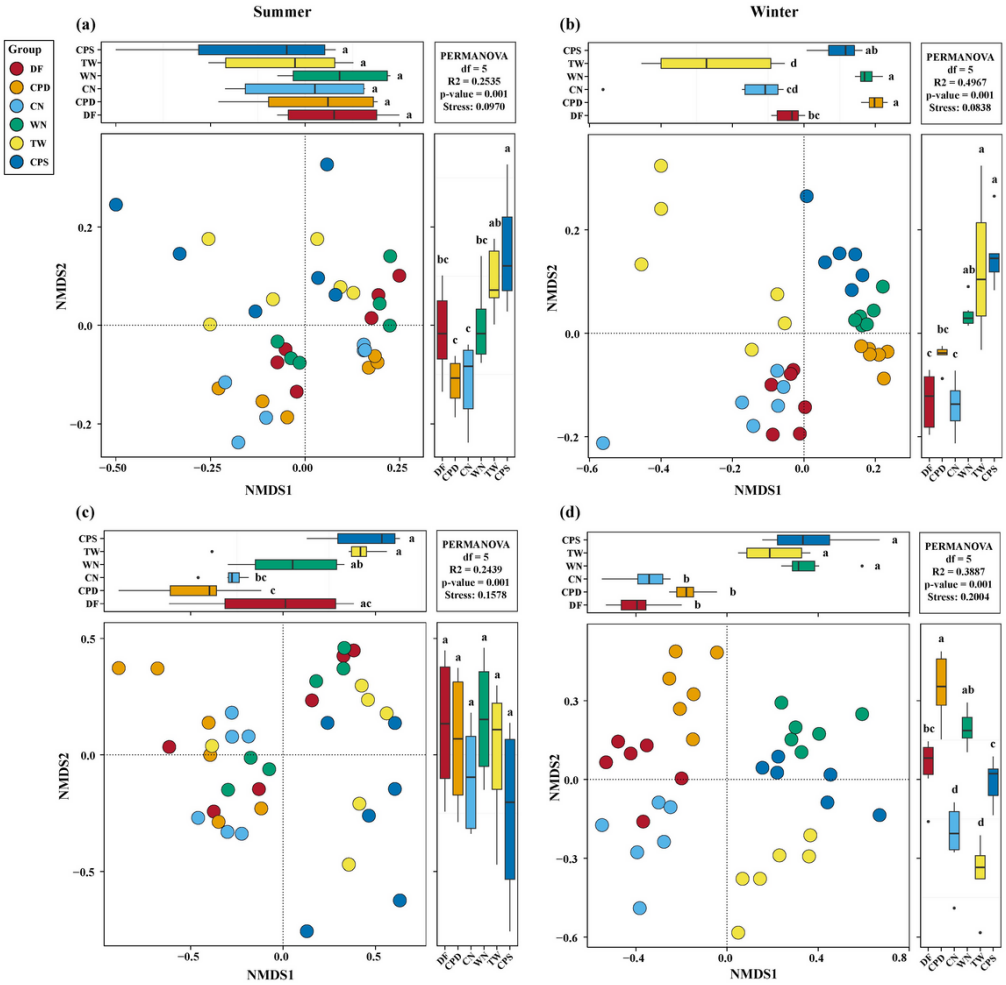

Figure 3

For both bacteria and fungi, the vegetation type led to significant differences in community composition (Fig. 3, $P < 0.001$), and there was a little overlap among the six vegetation types in summer (Fig. 3a and c). The bacterial and fungal community structures changed from summer (Fig. 3a and c) to winter (Fig. 3b and d), and the tighter clustering can be seen in the bar plots in Fig. 3. Due to their greater artificial disturbance, the Bray-Curtis distance between DF and CN was closer than among the other vegetation types, especially in winter (Fig. 3b and d). Meanwhile, the distance between CPD and CPS was greater than that between WN and CPS due to locational differences in Chinese pepper planting. Therefore, the effect of vegetation type on the composition of the bacterial and fungal communities was greater in winter than in summer, based on the larger PERMANOVA R2 values (Fig. 3).

Figure 4

The soil microbial network patterns differed among the six vegetation types and showed clear changes from summer to winter (Fig. 4a-l, Table S4). The microbial taxa showed higher network connectivity (i.e. network degree) under CN and CPD (Fig. 4c-f) than in other vegetation types. Bacterial taxa had higher network degrees than fungal taxa, especially under CN and CPD in winter (Fig. 4d, f, Table S4). In summer and winter, the average number of nodes under CN (641) was lower than under the other vegetation types (DF 764, CPD 754, WN 746, CPS 734, TW 660), while the average number of links under CN (2333) was lower than under CPD (2764), but higher than under the other vegetation types (Fig. 4, Table S4). The average path distances under CN (5.917) and CPD (5.809) were lower than under the other vegetation types, with values > 7 (Table S4). Moreover, the proportion of negative network edges (mainly representing bacteria-fungi interkingdom correlations) sharply declined from 39.2% to 8.6% under CPD (Fig. 4c, d) and from 40.3% to 8.8% under CN (Fig. 4e, f) from summer to winter, respectively.

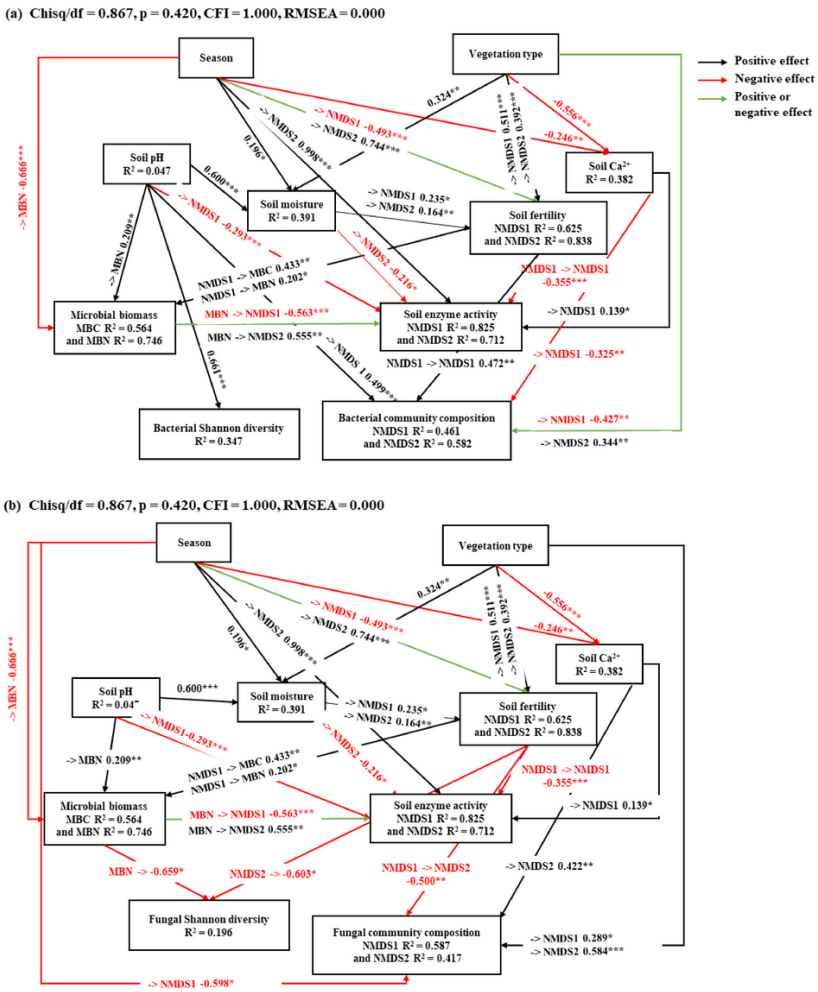

Figure 5

Thirty-five percent of the variance in the bacterial Shannon diversity index was explained by soil pH alone (Fig. 5a, path coefficient = 0.661***). The SEM explained 46% and 58% of the variance in the first and second bacterial community NMDS axes. Soil pH and fertility showed direct positive effects, whereas vegetation type and soil Ca2+ showed direct negative effects on bacterial community NMDS1. Vegetation type directly and positively influenced bacterial community NMDS2. Due to direct and indirect effects mediated by soil fertility, vegetation type showed a stronger effect on bacterial community composition than soil pH and Ca2+. The fungal Shannon diversity index was directly and negatively influenced by MBN (-0.659) and soil fertility NMDS2 (0.603) (Fig. 5b).

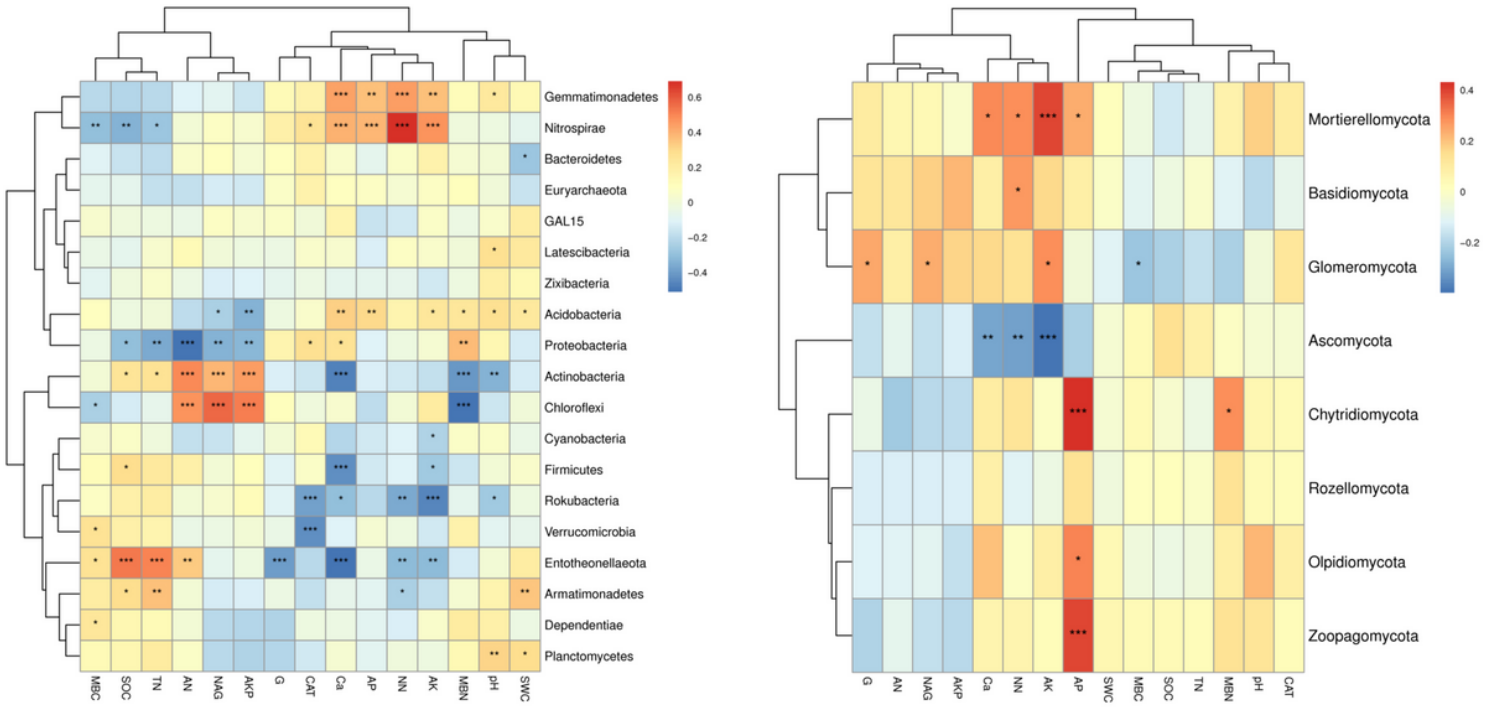

Figure 6

For bacterial phyla, the SOC and TN contents showed significant and positive correlations with the abundances of Entotheonellaeota, Armatimonadetes, and Actinobacteria ($P < 0.05$), but were negatively correlated with the abundances of Nitrospirae and Proteobacteria (Fig. 6a, $P < 0.05$). The soil Ca2+, AP, AK, and NO3–N contents were positively correlated with Nitrospirae and Gemmatimonadetes: in particular, the NO3–N content was strongly significantly correlated with them ($r = 0.69$, $P < 0.001$). Meanwhile, the soil Ca2+ content was negatively correlated with the abundances of Actinobacteria, Entotheonellaeota, and Firmicutes ($r < -0.4$, $P < 0.001$). The soil NH4+-N content, and the AKP and NAG enzyme activities, were positively correlated with the abundance of Actinobacteria and Chloroflexi, but negatively correlated with the abundance of Proteobacteria. CAT enzyme activity was negatively correlated with the abundance of Rokubacteria and Verrucomicrobia, while the activity of glucosidase was negatively correlated with the abundance of Entotheonellaeota. For the fungal phyla, the soil Ca2+, AP, AK, and NO3–N contents were positively correlated with the abundance of Mortierellomycota (Fig. 6b, $P < 0.001$). However, the soil Ca2+, AK, and NO3–N contents showed significant and negative correlations with the abundance of Ascomycota ($P < 0.01$). The soil AP content was positively correlated with the abundances of Chytridiomycota and Zoopagomycota. Glycosidase and NAG activities were positively correlated with the abundance of Glomeromycota.

Supplementary Files

This is a list of supplementary files associated with this preprint. Click to download.

- Supplementarymaterials.docx